International Journal of Natural Resources and Environmental Studies
ISSN: 3006-2012 (Print), ISSN: 3006-0834 (Online) | Volume 5, Number 2, Year 2025
DOI: https://doi.org/10.62051/ijnres.v5n2.18
Journal homepage: https://wepub.org/index.php/IJNRES/index

Prediction of Gas Emission in Mining Face Based on GRA-ISA-LSSVM

Xiong Huang[1, 2, *], Changsheng Shi[1], Yuepeng Yan[2]

[1]Huainan Vocational Technical College, Huainan, 232001 China;

[2]Anhui University of Science and Technology, Huainan, 232001 China.

*Corresponding Author: Xiong Huang

ABSTRACT

Coal, as a crucial primary energy source in China, provides a stable energy supply and security for the nation's economic and sustainable high-quality development. However, gas disasters can lead to severe casualties and significant economic losses. Therefore, accurately and efficiently predicting gas emission is of paramount importance and holds significant practical value for the safe production of high-gas mines. This paper employs the Least Squares Support Vector Machine (LSSVM) model, which offers better regression prediction accuracy for nonlinear problems with small datasets. To enhance the model's prediction accuracy and effectiveness, the Grey Relational Analysis (GRA) method is used to analyze the influencing factors of gas emission. Factors with high correlation are selected as model inputs. Experimental results show that coal seam gas content, coal seam depth, coal seam thickness, adjacent seam gas content, adjacent seam spacing, mining face length, and adjacent seam thickness have high correlation. To validate the results, Kendall's tau-b, Pearson, and Spearman correlation analysis methods are used, and the experimental results align with GRA. Genetic Algorithm (GA), Particle Swarm Optimization (PSO), and Improved Simulated Annealing Algorithm (ISA) are employed to find the global optimal solution for the LSSVM model parameters. Finally, the GRA-GA-LSSVM, GRA-PSO-LSSVM, and GRA-ISA-LSSVM models are constructed and tested. Experimental results show that after applying GRA, the RMSE and MAE metrics decrease, while the R^2 metric increases, proving that the GRA method optimizes the model. The GRA-ISA-LSSVM model has the lowest RMSE and MAE values and the highest R^2 value, indicating superior performance in static gas emission prediction.

KEYWORDS

Gas emission prediction; Grey Relational Analysis; GRA-ISA-LSSVM.

1. INTRODUCTION

Currently, most coal mines in China operate at depths exceeding 600 meters. Under these conditions, the risk of gas concentration exceeding safety limits in fully mechanized mining faces increases. When gas concentration surpasses the safety threshold, it can lead to gas accidents, affecting mining progress and causing casualties. Therefore, domestic and international experts have made significant achievements in gas emission prediction technology, studying gas emission patterns from various dimensions and constructing prediction models to improve accuracy and effectiveness. In traditional prediction methods, Dunmore R[1]proposed a practical method for predicting gas emissions based on initial gas content, working depth, source thickness, mining area age, and expected emission levels. Lunarzewski L [2] emphasized the importance of gas drainage in ensuring mine safety and proposed a gas emission model. Noack K [3]improved gas emission control in mining faces using large-diameter boreholes and introduced a method for predicting gas emissions in mining faces. Karacan C

O [4] used geostatistical methods to predict gas emissions in mining faces. Airey [5] identified time and mining technology as significant factors influencing gas emissions. In single-model prediction studies, Dong [6] used Gaussian theory to construct a regression model for time-series gas emission prediction, improving accuracy. Pan [7] built a wavelet neural network model based on time-series gas emission data to predict future gas emissions. In combined model prediction studies, Lu [8] used Principal Component Analysis (PCA) for data dimensionality reduction and employed a BP neural network model for gas emission prediction, showing improved accuracy after dimensionality reduction. Feng [9] combined a time-varying particle swarm algorithm with LSSVM, demonstrating improved prediction effectiveness. This paper uses the LSSVM model, which offers better regression prediction accuracy for nonlinear problems with small datasets. To enhance prediction accuracy and effectiveness, the GRA-ISA-LSSVM model is constructed and tested on the absolute gas emission data of a mining face in the Qianjiaying mining area of the Kailuan Mining Group, providing guidance for new mining levels.

2. THEORETICAL MODEL AND PARAMETER SETTINGS

2.1. Determination of Gas Emission Prediction Indicators

2.1.1. Grey Relational Analysis

GRA was first proposed by Professor Deng Julong in 1984. It analyzes system factors, uncovers potential relationships between data, and determines the degree of influence, improving mathematical statistical analysis methods. GRA is applicable regardless of sample size or regularity [10]. Gas emission is a grey system with partially known and unknown information. Therefore, GRA is used to analyze the influencing factors of gas emission and quantify their impact.

1.Select several influencing factors of gas emission. The feature vector of the i-th sample and the feature vector of the sample to be predicted are as follows:

$$Y_i = [\, y_{i1} \quad y_{i2} \quad y_{i3} \quad \cdots \quad y_{im} \,] \tag{1}$$

$$Y_0 = [\, y_{01} \quad y_{02} \quad y_{03} \quad \cdots \quad y_{0m} \,] \tag{2}$$

Where:

y_{im} — The feature value of the m-th influencing factor of the i-th sample;

y_{om} — The feature value of the m-th influencing factor of the sample to be predicted.

2.Normalize the feature values of the k-th influencing factor of the k-th sample and the sample to be predicted, calculate the difference sequence, and determine the maximum and minimum differences, as shown in equation (3):

$$T_{ik} = \frac{\min\limits_{i=1,\cdots,n} \min\limits_{k=1,\cdots,m} |y_{0k} - y_{ik}| + \rho \max\limits_{i=1,\cdots,n} \max\limits_{k=1,\cdots,m} |y_{0k} - y_{ik}|}{|y_{0k} - y_{ik}| + \rho \max\limits_{i=1,\cdots,n} \max\limits_{k=1,\cdots,m} |y_{0k} - y_{ik}|} \tag{3}$$

Where:

T_{ik} — The correlation coefficient of the k-th influencing factor of the i-th sample;

ρ — The resolution coefficient.

3.Use the correlation coefficient method to determine the weight of the k-th influencing factor, and construct the feature vector of each influencing factor's weight, as shown in equations (4) and (5):

$$\omega_k = \frac{p_k}{\sum_{k=1}^{m} p_k} \tag{4}$$

$$W = [\omega_1 \quad \omega_2 \quad \cdots \quad \omega_m] \tag{5}$$

Where:

P_k — The absolute value of the grey correlation coefficient of the k-th influencing factor;

ω_k — The weight of the k-th influencing factor.

4.Construct the grey correlation judgment matrix as shown in equation (6), and weight it with equation (5) to obtain the weighted grey correlation decision matrix as shown in equation (7):

$$T = \begin{bmatrix} T_{11} & T_{12} & T_{13} & \cdots & T_{1m} \\ T_{21} & T_{22} & T_{23} & \cdots & T_{2m} \\ \vdots & \vdots & \vdots & \vdots & \vdots \\ T_{n1} & T_{n2} & T_{n3} & \cdots & T_{nm} \end{bmatrix} \tag{6}$$

$$T' = TW^{\mathrm{T}} = \begin{bmatrix} \omega_1 T_{11} & \omega_2 T_{12} & \omega_3 T_{13} & \cdots & \omega_m T_{1m} \\ \omega_1 T_{21} & \omega_2 T_{22} & \omega_3 T_{23} & \cdots & \omega_m T_{2m} \\ \vdots & \vdots & \vdots & & \vdots \\ \omega_1 T_{n1} & \omega_2 T_{n2} & \omega_3 T_{n3} & \cdots & \omega_m T_{nm} \end{bmatrix} \tag{7}$$

5.Calculate the grey correlation degree of the i-th sample, as shown in equation (8):

$$D_i = \sum_{k=1}^{m} \omega_k T_{ik} \tag{8}$$

Where:

D_i — The grey correlation degree of the i-th sample.

2.1.2. Analysis of Gas Emission Influencing Factors Based on GRA

Relevant scholars have made significant contributions to the study of gas emission influencing factors. Based on [10] and expert and field technician evaluations, this paper summarizes the influencing factors of gas emission and uses the original data as the training and testing samples for the regression prediction model, as shown in Table 1.

Table 1. Regression prediction model training and testing samples

No.	Coal Seam Gas Content(m^3•t-1)	Depth (m^3•t-1)	Coal Seam Thicknessm	Coal Seam Dip Angle (º)	Daily Progress(m)	Mining Face Length (m)	Recovery Rate	Adjacent Seam Gas Content (m^3/t)	Adjacent Seam Thickness (m)	Adjacent Seam Spacing (m)	Interlayer Lithology	Gas Emission (m^3/min)
1	1.92	408	2	10	4.42	155	0.96	2.02	1.5	20	5.03	3.34
2	2.14	421	1.8	11	4.13	145	0.95	2.64	1.62	19	4.75	3.56
3	2.58	450	2.3	10	4.67	150	0.95	2.41	1.48	18	4.91	3.67
4	2.4	456	2.2	15	4.51	160	0.94	2.55	1.75	20	4.63	4.17
5	3.22	516	2.8	13	3.45	180	0.93	2.21	1.72	12	4.78	4.6
6	2.8	527	2.5	17	3.28	180	0.94	2.81	1.81	11	4.51	4.92
7	3.23	517	2.8	13	3.46	180	0.93	2.23	1.71	12	4.76	4.61
8	3.35	531	2.9	9	3.68	165	0.93	1.88	1.42	13	1.82	4.78
9	3.61	550	2.9	12	4.02	155	0.92	2.12	1.60	14	4.83	5.23
10	3.71	573	3.2	11	2.92	175	0.91	3.11	1.46	13	4.63	5.62
11	4.21	590	5.9	8	2.85	170	0.79	3.4	1.5	18	4.77	7.24
12	4.03	604	6.2	9	2.64	180	0.81	3.15	1.8	16	4.70	7.8
13	4.8	630	6.5	9	2.77	165	0.78	3.02	1.74	17	4.62	7.68
14	4.67	640	6.3	11	2.75	175	0.80	2.56	1.75	15	4.6	7.95
15	2.43	450	2.7	11	4.32	165	0.93	2.35	1.85	16	4.58	5.06
16	3.16	544	2.7	17	3.81	165	0.93	2.81	1.79	13	4.9	4.93
17	4.62	629	6.4	13	2.8	170	0.80	3.35	1.61	19	4.63	8.04
18	4.53	635	6.2	9	2.73	160	0.71	2.94	1.73	17	4.61	7.56
19	3.87	580	3.9	11	2.85	170	0.92	3.02	1.39	14	4.72	5.82
20	3.24	509	2.5	14	4.4	160	0.93	2.79	1.72	13	4.65	4.36

In Table 1, the reference data column consists of the influencing factors of gas emission, while the comparison data column is the gas emission volume. The feature vectors of the reference and comparison data are determined using Equations (1) to (2). The elements of the comparison data feature vector are normalized to make the reference and comparison data comparable. The difference sequence, maximum and minimum differences, and correlation coefficients are calculated as shown in Table 2. Based on the correlation coefficient values, the final correlation degree values are obtained and illustrated in Figure 3.

Table 2. Correlation coefficient results

No.	Coal Seam Gas Content (m^3/t)	Depth (m)	Coal Seam Thickness (m)	Coal Seam Dip Angle (°)	Daily Progress (m)	Mining Face Length (m)	Recovery Rate	Adjacent Seam Gas Content (m^3/t)	Adjacent Seam Thickness (m)	Adjacent Seam Spacing (m)	Interlayer Lithology
1	0.89	0.69	0.84	0.57	0.35	0.51	0.42	0.69	0.53	0.33	0.41
2	0.95	0.71	0.68	0.53	0.39	0.60	0.45	0.50	0.50	0.37	0.46
3	0.79	0.66	0.88	0.64	0.34	0.59	0.46	0.59	0.59	0.41	0.46
4	0.87	0.78	0.68	0.39	0.39	0.62	0.53	0.63	0.53	0.39	0.57
5	0.76	0.73	0.81	0.55	0.70	0.58	0.61	1.00	0.62	0.86	0.61
6	0.83	0.79	0.61	0.38	0.89	0.64	0.67	0.67	0.62	0.66	0.78
7	0.76	0.73	0.81	0.55	0.70	0.58	0.62	0.99	0.62	0.86	0.62
8	0.75	0.73	0.80	0.79	0.65	0.73	0.65	0.69	1.00	0.94	0.43
9	0.76	0.81	0.67	0.80	0.63	0.97	0.79	0.70	0.92	0.90	0.75
10	0.83	0.87	0.69	0.83	0.65	0.90	0.97	0.69	0.73	0.66	1.00
11	0.82	0.62	0.56	0.36	0.41	0.55	0.46	0.92	0.47	0.71	0.57
12	0.60	0.55	0.58	0.35	0.34	0.52	0.41	0.60	0.52	0.48	0.48
13	0.95	0.62	0.49	0.36	0.37	0.47	0.41	0.58	0.51	0.54	0.48
14	0.83	0.59	0.58	0.41	0.35	0.48	0.39	0.42	0.48	0.43	0.45
15	0.63	0.82	0.65	0.92	0.52	0.81	0.72	0.92	0.62	0.74	0.79
16	0.91	0.74	0.68	0.38	0.64	0.77	0.69	0.68	0.64	0.87	0.65
17	0.77	0.55	0.57	0.51	0.34	0.45	0.39	0.64	0.42	0.61	0.44
18	0.89	0.65	0.54	0.37	0.37	0.46	0.38	0.57	0.52	0.56	0.49
19	0.81	0.92	0.99	0.77	0.59	0.93	0.96	0.81	0.63	0.70	0.95
20	0.68	0.68	0.75	0.45	0.43	0.66	0.57	0.57	0.57	0.87	0.60

From Table 2, the grey correlation analysis of 11 evaluation items (coal seam gas content, depth, coal seam thickness, coal seam dip angle, daily progress, mining face length, recovery rate, adjacent seam gas content, adjacent seam thickness, adjacent seam spacing, interlayer lithology) and 20 data items is conducted, with gas emission as the "reference value" (parent sequence). The correlation between the 11 evaluation items and gas emission (correlation degree) is studied.

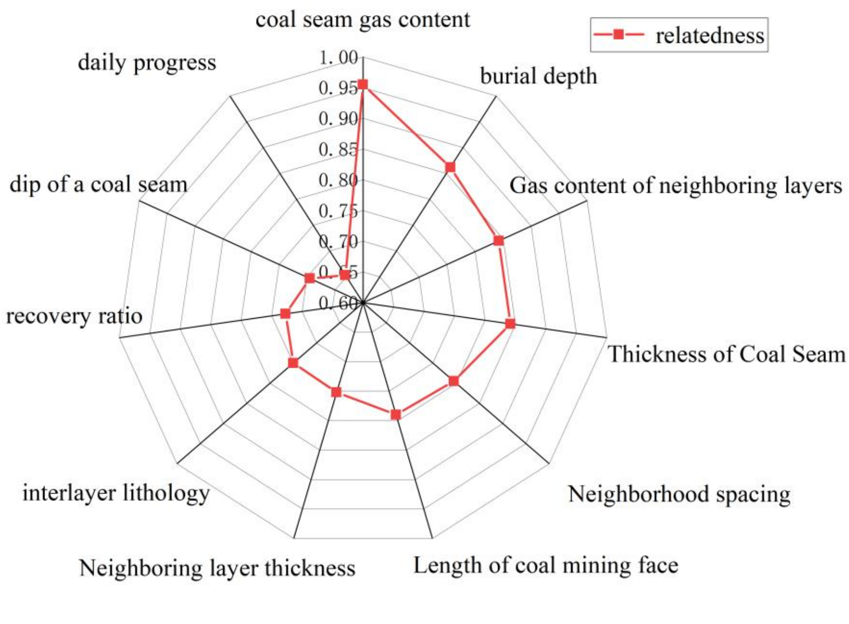

Fig 1. Relatedness

From Figure 1, the correlation degree values are in the range (0,1). The larger the value, the stronger the correlation between the evaluation item and gas emission (parent sequence), and the higher the correlation degree. Based on the correlation degree values of the 11 evaluation items, those exceeding 0.75 are selected as inputs for the regression prediction model, namely coal seam gas content (0.955), depth (0.862), coal seam thickness (0.842), adjacent seam gas content (0.841), adjacent seam spacing (0.795), mining face length (0.790), and adjacent seam thickness (0.752).

2.1.3. Correlation Analysis Verification

To verify the high-correlation influencing factors identified by GRA, Kendall's tau-b, Pearson, and Spearman correlation analysis methods are used to analyze the influencing factors of gas emission, as shown in Figures 2-4.

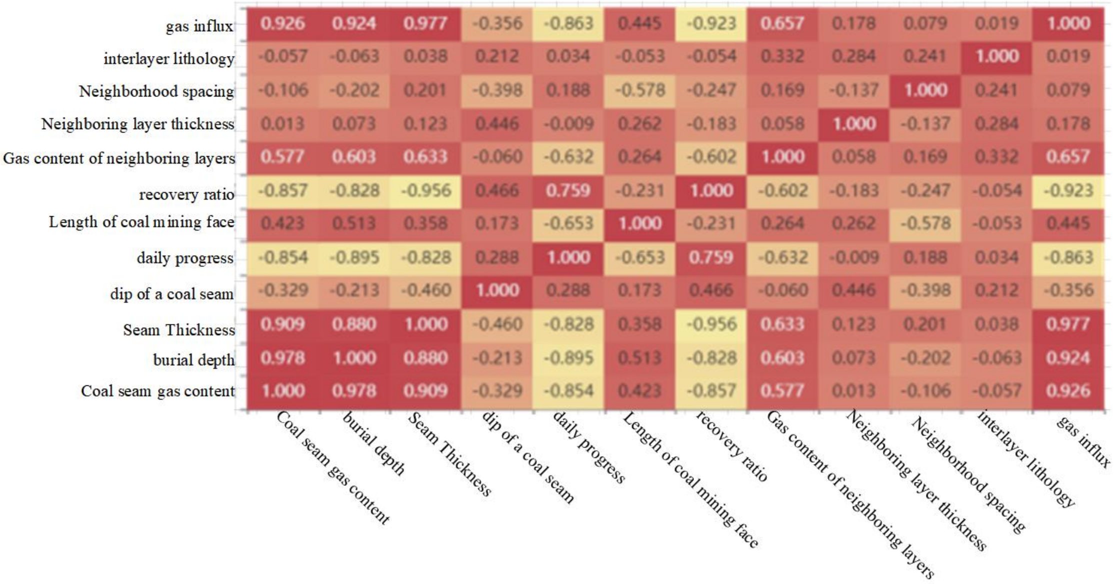

Fig 2. Pearson correlation analysis

From Figure 2, gas emission has higher correlation with coal seam thickness (0.977), coal seam gas content (0.926), depth (0.924), adjacent seam gas content (0.657), mining face length (0.445), adjacent seam thickness (0.178), and adjacent seam spacing (0.079), consistent with GRA results.

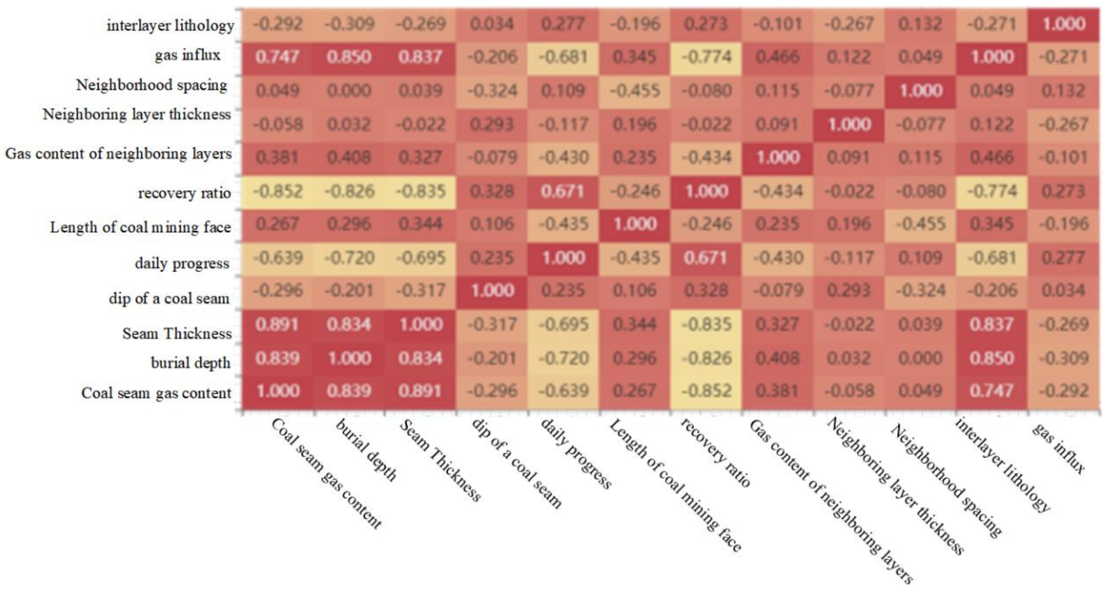

Fig 3. Kendall's tau-b correlation analysis

From Figure 3, gas emission has higher correlation with depth (0.85), coal seam thickness (0.837), coal seam gas content (0.747), adjacent seam gas content (0.466), mining face length (0.345), adjacent seam thickness (0.122), and adjacent seam spacing (0.049), consistent with GRA results.

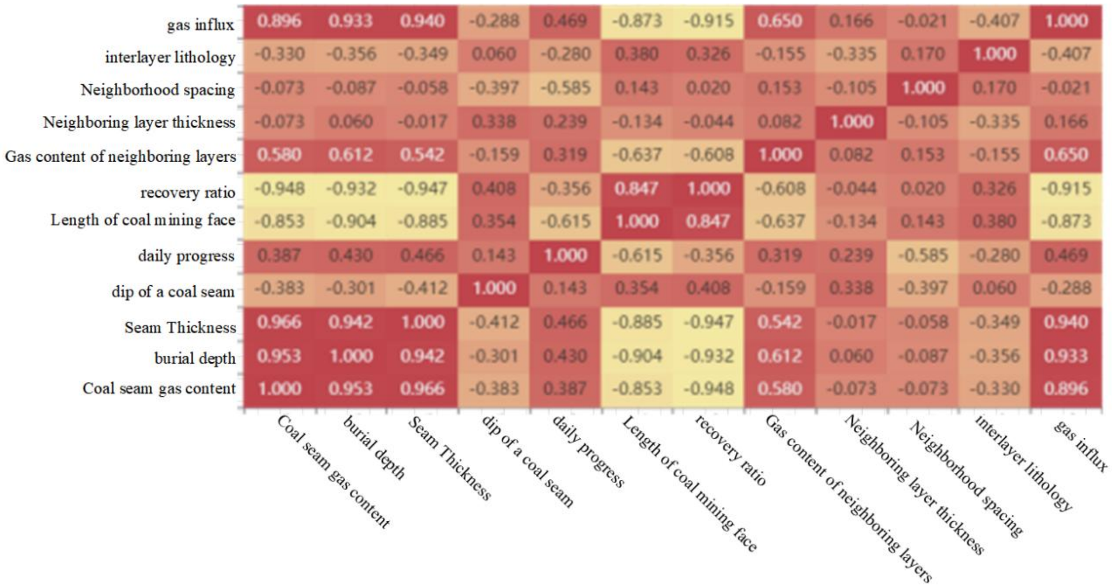

Fig 4. Spearman correlation analysis

From Figure 4, gas emission has higher correlation with coal seam thickness (0.940), depth (0.933), coal seam gas content (0.896), adjacent seam gas content (0.650), mining face length (0.469), adjacent seam thickness (0.116), and adjacent seam spacing (-0.021), consistent with GRA results.

2.2. Construction of Gas Emission Prediction Model Based on GRA-ISA-LSSVM

2.2.1. Improved Simulated Annealing Algorithm

Based on the traditional SA algorithm's acceptance probability method and Metropolis criterion, a functional module is constructed to separate target optimization and constraint satisfaction, incorporating a tempering operation and global search model perturbation strategy to improve algorithm efficiency and solve for the global optimal solution, as shown in Figure 5.

The ISA algorithm framework uses a random generator to generate new solutions, improving efficiency compared to the traditional SA algorithm's fixed-step perturbation search for the optimal solution. During high-temperature annealing, global search enhances solution accuracy and locks in the optimal solution. The random global perturbation strategy is shown in equation (9):

$$\boldsymbol{X}_i = \boldsymbol{a}_i + \boldsymbol{m} \cdot (\boldsymbol{b}_i - \boldsymbol{a}_i) \tag{9}$$

Where:

X_i——The new solution model generated by random perturbation;

b_i——The upper bound of model perturbation;

a_i——The lower bound of model perturbation;

μ——The perturbation coefficient of the model random generator.

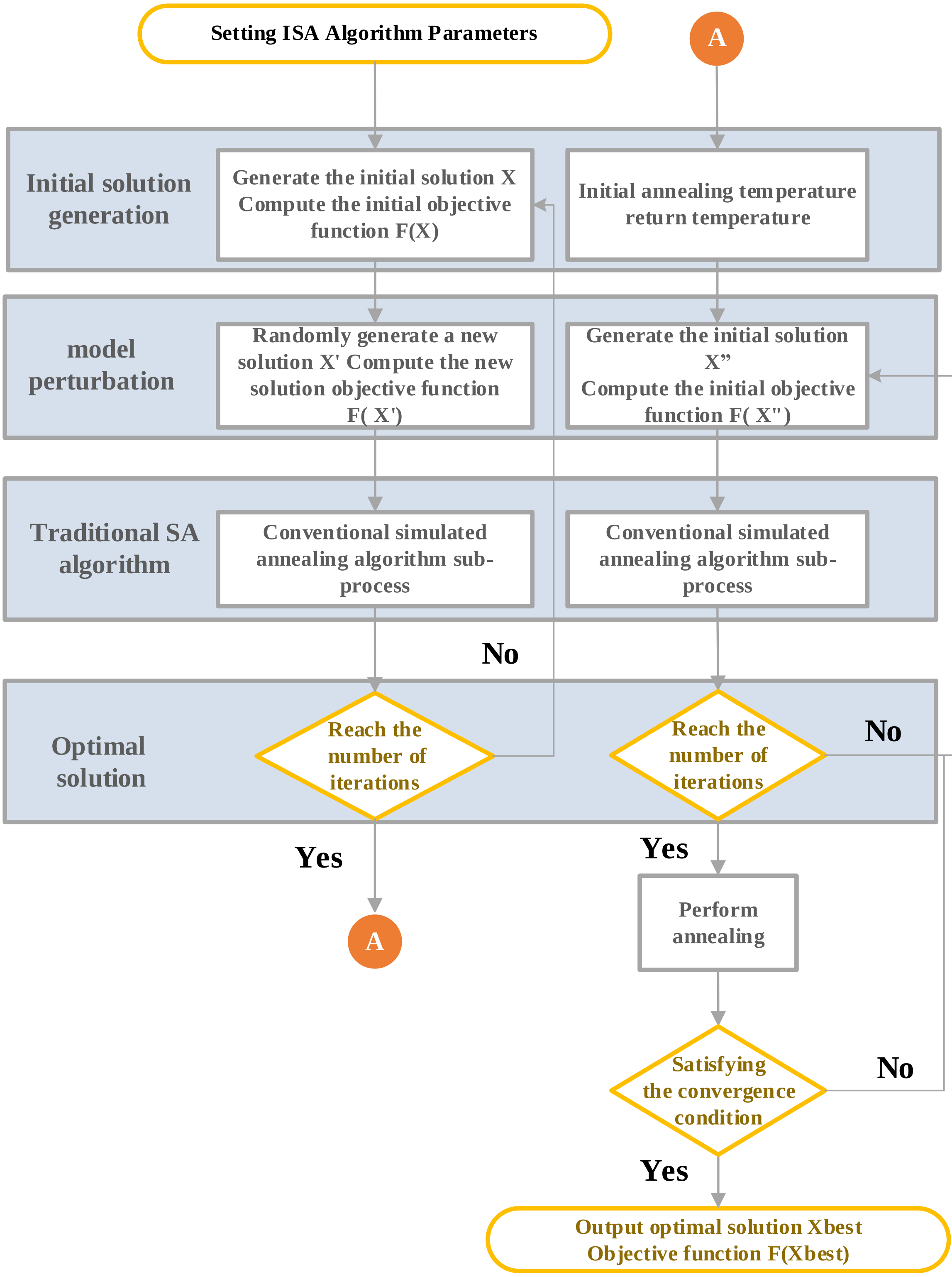

Fig 5. ISA algorithm construction framework diagram

Based on the ISA algorithm framework, MATLAB is used for simulation and solution. The ISA algorithm implementation process is shown in Figure 6.

The ISA algorithm calculation steps are as follows: Step 1: Initialize ISA algorithm parameters and generate the initial solution; Step 2: Use the global search model perturbation strategy to randomly generate a new solution and calculate the new solution's objective function; Step 3: Compare the new solution's objective function value with the initial solution's objective function value. If the new solution's value is smaller, accept the new solution state; otherwise, accept the new solution according to the Metropolis criterion; Step 4: Check if the iteration count is reached. If so, perform the tempering operation; otherwise, return to Step 2; Step 5: Perform the tempering operation to generate the initial solution and calculate the objective function value. Compare it with the original objective function value. If the new value is smaller, accept the new solution state; otherwise, accept the new solution according to the Metropolis criterion; Step 6: Check if the iteration count is reached. If so, perform the tempering operation; otherwise, return to Step 5; Step 7: Perform annealing and check if the convergence condition is met. If so, output the optimal solution; otherwise, return to Step 5.

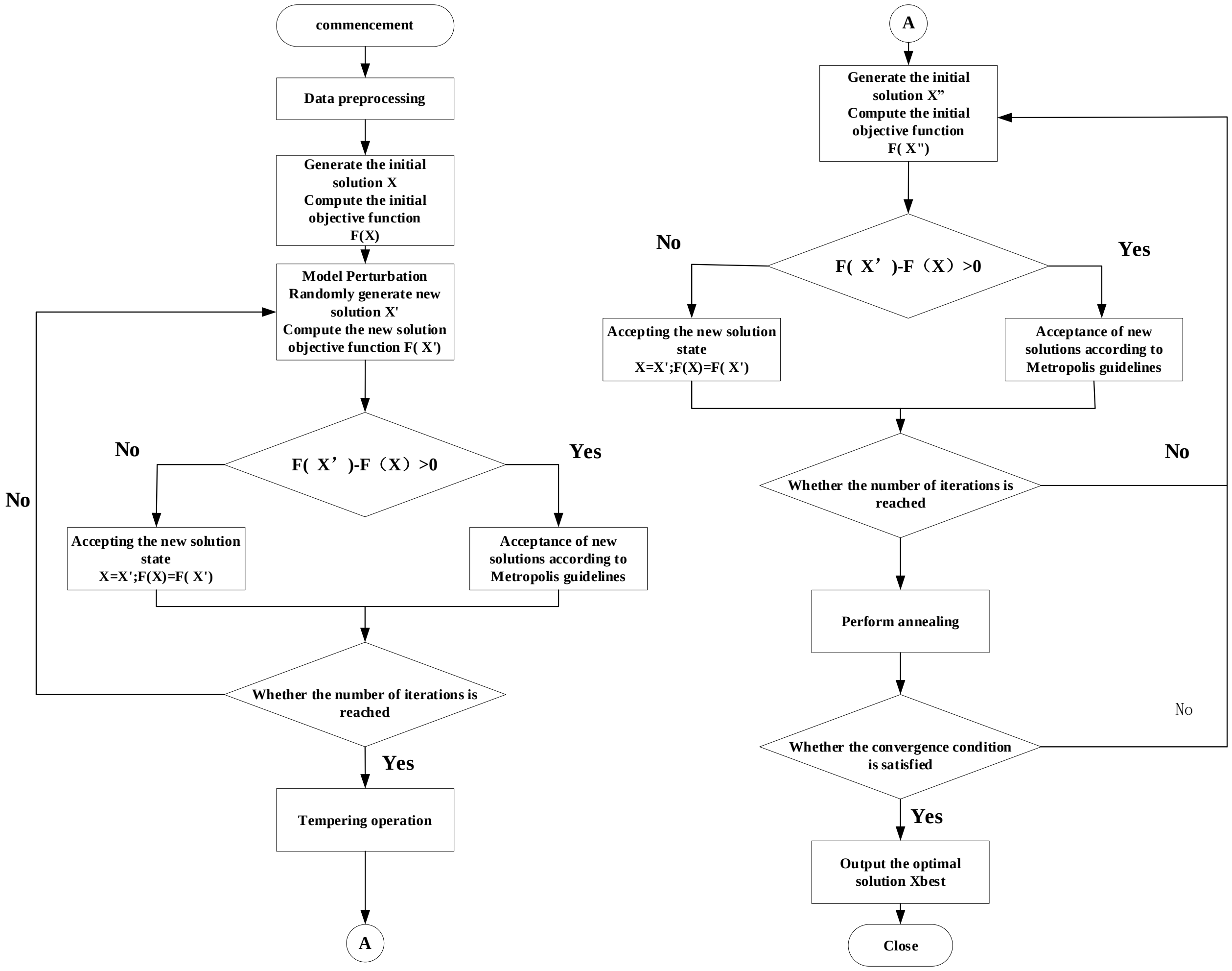

Fig 6. Flow chart of ISA algorithm

During the annealing iteration, the tempering operation is introduced to help the solution escape local optima and improve solution accuracy. When the annealing iteration reaches the final temperature, the tempering factor increases the temperature for the tempering operation, enhancing the ISA algorithm's ability to search for suboptimal solutions and escape local optima, ultimately improving solution accuracy. The tempering operation flow is shown in Figure 7.

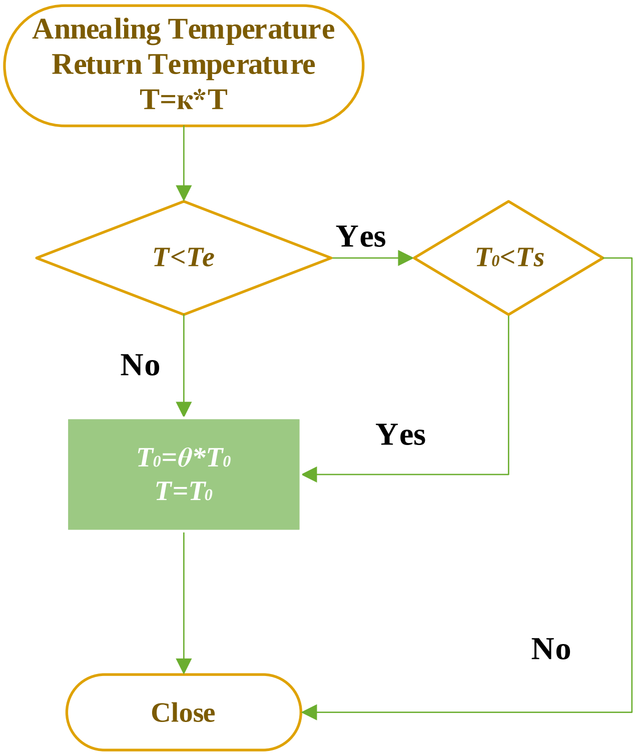

Fig 7. Tempering operation flow block diagram

In Figure 7, k represents the annealing factor; θ is the tempering factor; T_0 is the annealing start temperature;

T_s is the tempering end temperature; T_e is the annealing termination temperature.

2.2.2. GRA-ISA-LSSVM Prediction Model

First, the GRA method is used to select high-correlation influencing factors. Then, the ISA algorithm is used to automatically optimize LSSVM model parameters. Finally, the GRA-ISA-LSSVM model is constructed, as shown in Figure 8.

The GRA-ISA-LSSVM model calculation steps are as follows:Step 1: Collect sample data and preprocess it (e.g., normalization);Step 2: Use GRA to analyze the sample data's correlation degree, obtain high-correlation influencing factor data, and divide it into training and testing sets as model inputs, with gas emission as the model output;Step 3: Randomly initialize LSSVM and ISA parameters;Step 4: Use the global search model perturbation strategy to randomly generate a new solution and calculate the new solution's objective function;Step 5: Compare the new solution's objective function value with the initial solution's objective function value. If the new solution's value is smaller, accept the new solution state; otherwise, accept the new solution according to the Metropolis criterion;Step 6: Check if the iteration count is reached. If so, perform the tempering operation; otherwise, return to Step 4;Step 7: Perform annealing and check if the convergence condition is met. If so, output the optimal solution; otherwise, return to Step 6;Step 8: Use the optimal parameters (position and velocity) output by ISA as the LSSVM model's kernel width coefficient and penalty factor to build the model, and finally output the gas emission prediction results.

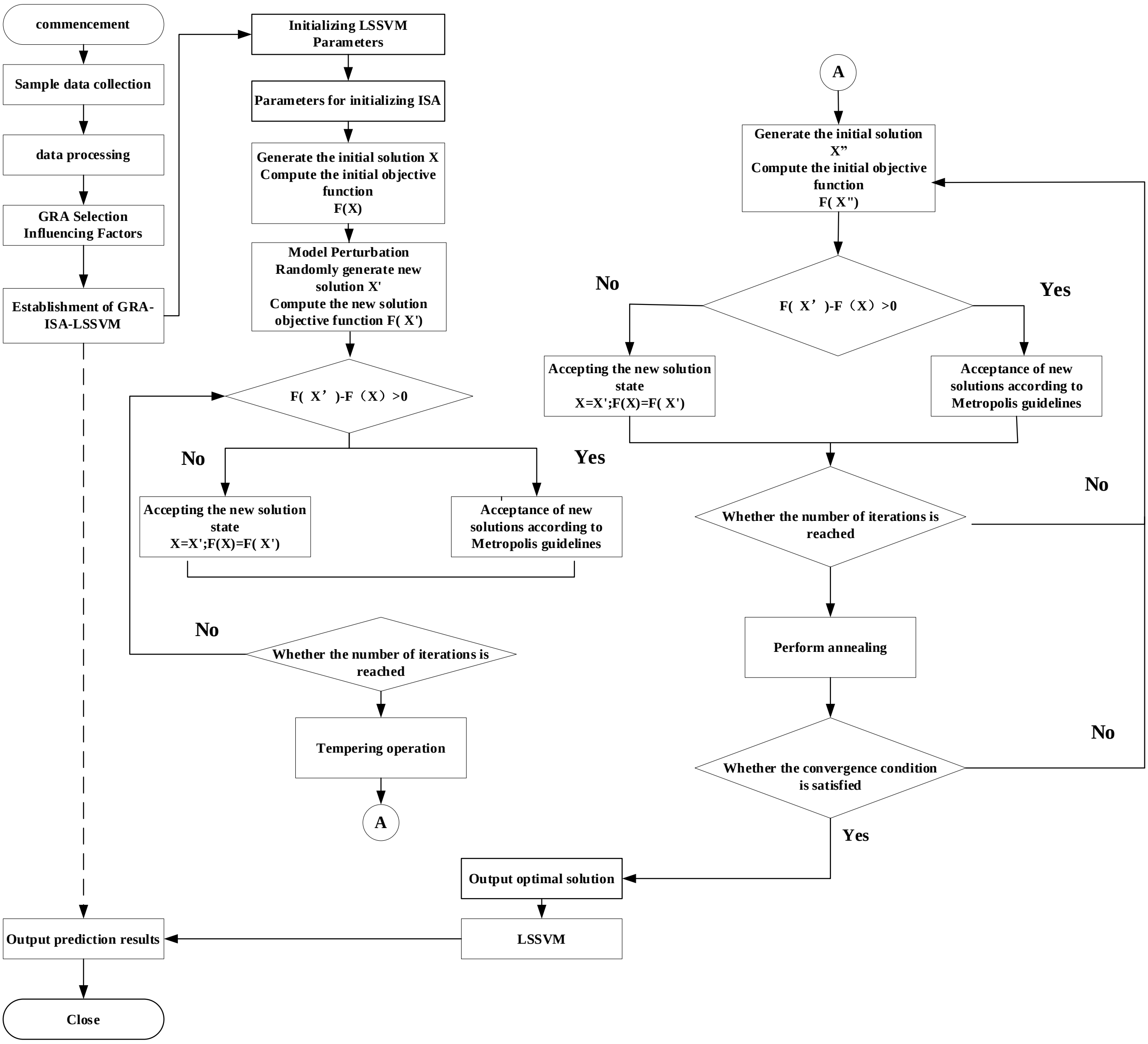

Fig 8. GRA-ISA-LSSVM model

3. SIMULATION RESULTS AND ANALYSIS

3.1. Comparison of Prediction Results from Different Algorithm-Optimized Models

Special Signs

Using the absolute gas emission data and influencing factors of a mining face in the Qianjiaying mining area of the Kailuan Mining Group as the experimental dataset, the GRA-GA-LSSVM, GRA-PSO-LSSVM, and GRA-ISA-LSSVM models are tested and compared to verify the algorithm's effectiveness. MATLAB is used for simulation experiments, and the training and prediction set results are shown in Figures 9-10.

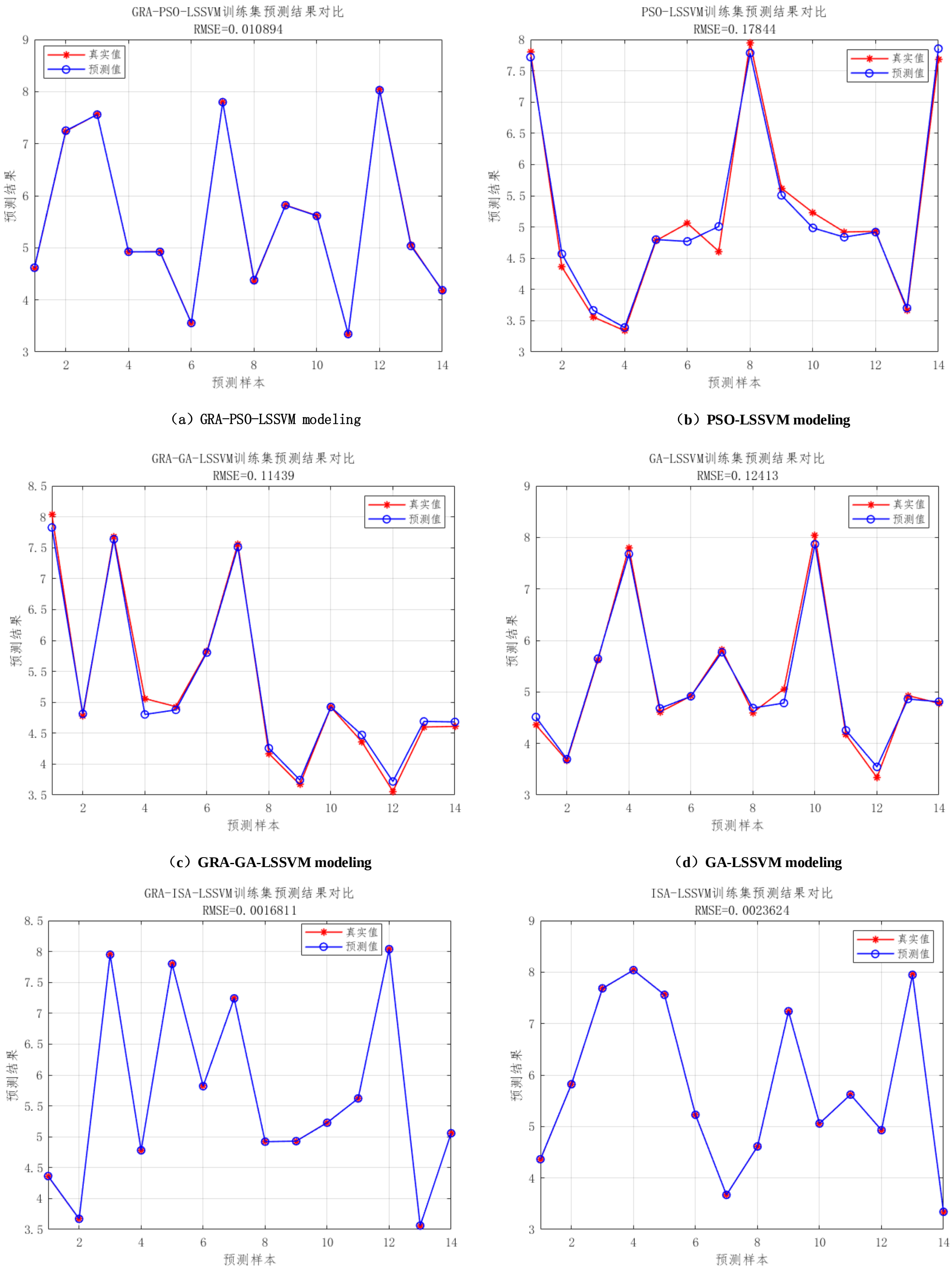

(a) GRA-PSO-LSSVM modeling

(b) PSO-LSSVM modeling

(c) GRA-GA-LSSVM modeling

(d) GA-LSSVM modeling

(e) GRA-ISA-LSSVM modeling

(f) ISA-LSSVM modeling

Fig 9. Training set prediction results

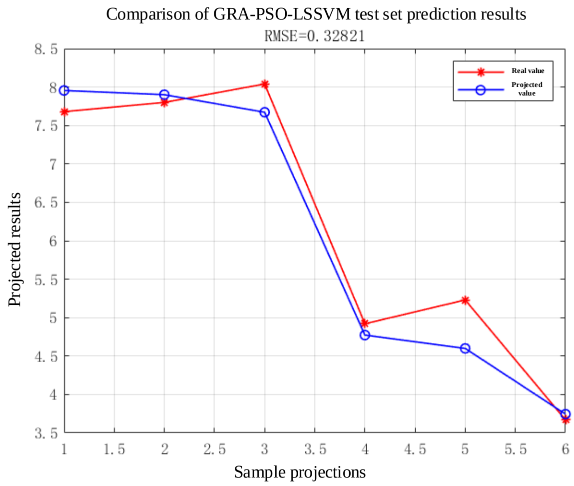

(a) GRA-PSO-LSSVM modeling

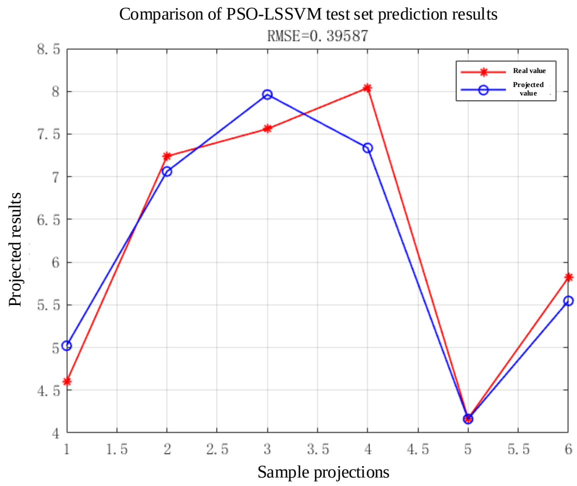

(b) PSO-LSSVM modeling

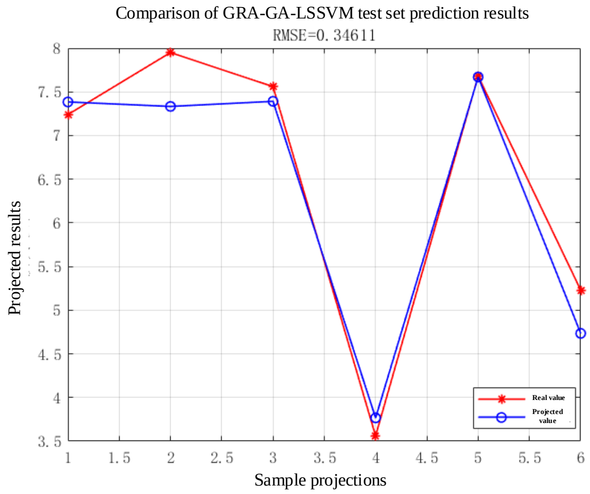

(c) GRA-GA-LSSVM modeling

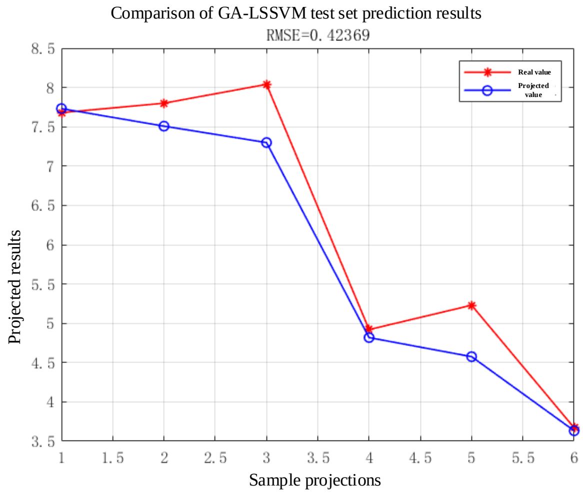

(d) GA-LSSVM modeling

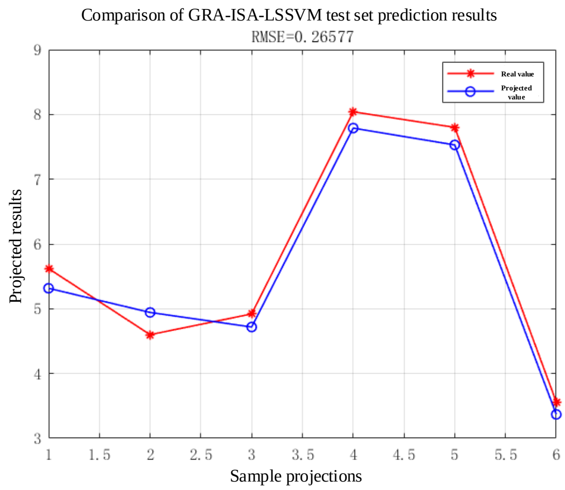

(e) GRA-PSO-LSSVM modeling

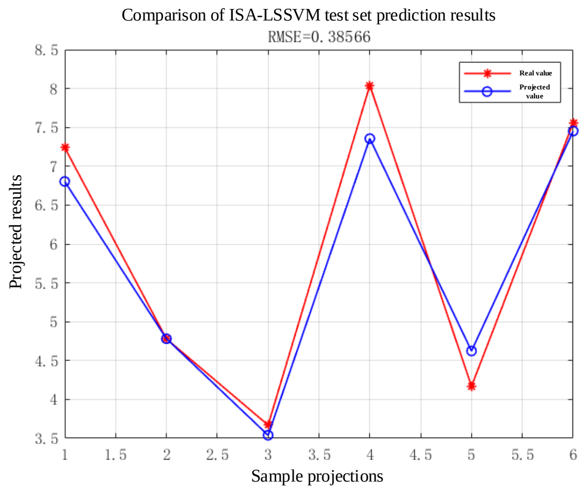

(f) PSO-LSSVM modeling

Fig 10. Test set prediction results

From Figures 9-10, the red "*" line represents the true values, and the blue "O" line represents the predicted values. After applying GRA, the model's prediction accuracy improves. The GRA-ISA-LSSVM model has the lowest RMSE value, indicating higher prediction accuracy and reliability.

3.2. Experimental Evaluation Metrics

The error evaluation metrics for the gas emission prediction model include Root Mean Square Error (RMSE), Mean Absolute Error (MAE), and the coefficient of determination R^2. The mathematical expressions for these metrics are as follows:

$$MAPE = \frac{100\%}{n}\sum_{i=1}^{n}\left|\frac{\hat{y}_i - y_i}{y_i}\right| \tag{10}$$

$$MAE = \frac{1}{n}\sum_{i=1}^{n}\left|\hat{y}_i - y_i\right| \tag{11}$$

$$RMSE = \frac{1}{n}\sqrt{\sum_{i=1}^{n}\left(\hat{y}_i - y_i\right)^2} \tag{12}$$

$$R^2 score\left(y,\hat{y}\right) = 1 - \frac{\sum_{i=1}^{n}\left(y_i - \hat{y}_i\right)^2}{\sum_{i=1}^{n}\left(y_i - \overline{y}\right)^2} \tag{13}$$

Where:

n —The number of test set samples;

y_i — The predicted gas concentration value;

$\hat{y}_i$ — The actual value.

Lower RMSE and MAE values indicate higher prediction accuracy, while a higher R^2 value indicates better model fit.

3.3. Experimental Analysis

This section tests the GRA-GA-LSSVM, GRA-PSO-LSSVM, and GRA-ISA-LSSVM models on the dataset and analyzes the error metrics, as shown in Table 3.

Table 3. Prediction model error indicators

Model	Training Set RMSE%			Test Set RMSE%		
	RMSE%	MAE	R2	RMSE%	MAE	R2
GRA-GA-LSSVM	11.44	0.07516	0.99137	34.61	0.42614	0.90346
GA-LSSVM	12.41	0.09831	0.99098	42.37	0.47031	0.89046
GRA-PSO-LSSVM	1.09	0.06912	0.99392	32.82	0.41983	0.90517
PSO-LSSVM	17.84	0.08342	0.99134	39.59	0.46197	0.88941
GRA-ISA-LSSVM	0.17	0.00187	0.99971	26.58	0.40181	0.91916
ISA-LSSVM	0.24	0.00213	0.99362	38.57	0.41708	0.90254
GRA-LSSVM	21.64	0.09461	0.85173	48.16	0.48319	0.88726
LSSVM	29.36	0.11038	0.83039	49.73	0.52264	0.86329

From Table 3, after applying GRA, the RMSE and MAE metrics decrease, and the R^2 metric increases, indicating improved prediction accuracy and model fit. Comparing the error metrics of the GRA-GA-LSSVM, GRA-PSO-LSSVM, GRA-ISA-LSSVM, and GRA-LSSVM models, the GRA-ISA-LSSVM model has the lowest RMSE and MAE values and the highest R^2 value. Compared to GRA-LSSVM, the training set RMSE and MAE values of GRA-ISA-LSSVM decrease by 21.59% and

0.09274, respectively, and the R^2 value increases by 0.14798. The test set RMSE and MAE values decrease by 21.48% and 0.08138, respectively, and the R^2 value increases by 0.03190, indicating superior gas emission prediction performance.

4. CONCLUSIONS AND DISCUSSIONS

1.Based on Grey Relational Analysis, the influencing factors of gas emission are analyzed, with coal seam gas content, coal seam depth, coal seam thickness, adjacent seam gas content, adjacent seam spacing, mining face length, and adjacent seam thickness showing high correlation. Kendall's tau-b, Pearson, and Spearman correlation analysis methods are used for verification.

2.The GRA-PSO-LSSVM, GRA-GA-LSSVM, and GRA-ISA-LSSVM models are constructed and tested. After applying GRA, the RMSE and MAE metrics decrease, and the R^2 metric increases, indicating improved prediction accuracy and model fit, proving that GRA optimizes the model. Comparing the error metrics of the GRA-GA-LSSVM, GRA-PSO-LSSVM, GRA-ISA-LSSVM, and GRA-LSSVM models, the GRA-ISA-LSSVM model has the lowest RMSE and MAE values and the highest R^2 value. Compared to GRA-LSSVM, the training set RMSE and MAE values of GRA-ISA-LSSVM decrease by 21.59% and 0.09274, respectively, and the R^2 value increases by 0.14798. The test set RMSE and MAE values decrease by 21.48% and 0.08138, respectively, and the R^2 value increases by 0.03190, indicating superior gas emission prediction performance.

ACKNOWLEDGEMENTS

2025 Huainan Vocational Technical College Natural Science Research Project "Research on Gas Emission Prediction Method Based on Machine Learning" (2025HZZK001); 2023 Anhui Provincial University Natural Science Research Project "Application Research on Gas Emission Prediction in Fully Mechanized Mining Face Based on Machine Learning" (2023AH053353); 2022 Huainan Vocational Technical College Natural Science Research Project "Research on Gas Emission Prediction Method in Fully Mechanized Mining Face Based on Machine Learning" (HKJ22-3)

REFERENCES

[1] R D. Prediction of gas emission from longwall faces[J]. Mining Engineering, 1981(140): 565-572.

[2] W L L L. Gas emission prediction and recovery in underground coal mines[J]. International Journal of Coal Geology, 1998, (1-4)(35): 117-145.

[3] K. N. Control of gas emissions in underground coal mines[J]. International Journal of Coal Geology, 1998,(1-4)(35): 57-82.

[4] KARACAN C Ö O R A G. Geostatistical modeling of the gas emission zone and its in-place gas content for Pittsburgh seam mines using sequential gaussian simulation[J]. International Journal of Coal, 2012(90): 50-71.

[5] M A E. Gas emission from broken coal. An experimental and theoretical investigation[J]. International Journal of Rock Mechanics & Mining Sciences & Geomechanics Abstracts, 1968,6(5): 475-494.

[6] DINGWEN D. Mine Gas Emission Prediction based on Gaussian Process Model[J]. [J]. Procedia Engineering, 2012(45): 334-338.

[7] PAN YUMIN D Y Z Q. Dynamic prediction of gas emission based on wavelet neural network toolbox[J]. [J]. Journal of Coal Science and Engineering, 2013,02(19): 174-181.

[8] LU GUOBIN K J B G. Application of PCA-BP to gas emission prediction of mining working face[J]. [J]. Journal of Liaoning Technical University, 2015,12(34): 1329-1334.

[9] FENG YUXI Z K Y X. Prediction for Gas Emission Quantity of the Working Face Based on LSSVM Optimized by Improved Particle Swarm Optimization[J]. [J]. Advanced Materials Research, 2014(1051): 1028-1031.

[10] Fu Hua, Xie Sen, Xu Yaosong, Chen Zichun. Research on dynamic prediction model of coal mine gas emission based on ACC-ENN algorithm [J]. Journal of China Coal Society, 2014, 39(07): 1296-1301.